

# Hydraulic lime mortars for the restoration of historic masonry in Crete

P. Maravelaki-Kalaitzaki<sup>a,\*</sup>, A. Bakolas<sup>b</sup>, I. Karatasios<sup>c</sup>, V. Kilikoglou<sup>c</sup>

<sup>a</sup>25th Ephorate of Prehistoric and Classical Antiquities, Chania, Ministry of Culture, 21 Chalidon Str., Chania 73100, Crete, Greece

<sup>b</sup>Department of Environmental Sciences, University of Venice, Calle Larga S. Marta 2137, Venice 30123, Italy

<sup>c</sup>Laboratory of Archaeometry, National Center for Scientific Research “Demokritos”, Agia Paraskevi, 15310 Attiki, Greece

Received 16 June 2004; accepted 1 September 2004

## Abstract

This study presents the results of the physico-chemical characterization of original mortars and plasters and the evaluation of the repair ones prepared with natural hydraulic lime (NHL) as binding material and siliceous sand and crushed brick as aggregates. The repair mortars were applied in restoration works of a historic masonry in Crete, Greece. The proportions of binder, aggregates and water were selected in order to achieve optimum workability. Original mortars, containing magnesian lime, had to be replaced since previous interventions with cement-based mortars have provoked damage acceleration. Water absorption by capillarity, compressive strength, modulus of elasticity, porosity and pore size distribution were determined at early stages and after 1 year of curing time; these properties prove the suitability of the proposed mortars for such an application. After 3 years of intervention with NHL-based mortars and plasters, macroscopic survey and analyses of the applied materials reveal that no cracks or release of soluble salts occur.

© 2004 Elsevier Ltd. All rights reserved.

**Keywords:** Magnesian lime mortars; Hydraulic lime mortars; Compatibility; Compressive strength; Water capillarity; Pore-size distribution

## 1. Introduction

In many of the historic masonries of Crete, Greece, parts of the original mortars, which have been deteriorated by natural weathering, need replacement. In most cases, restoration interventions had employed cement and polymer-based materials, which resulted in advancing the deterioration state, since harmful by-products have induced severe damage to the adjacent stone blocks [1]. In addition, the polymer-based materials are incompatible to the construction materials of the original masonries, thus exhibiting different behaviors in the environmental conditions. For this reason, the ongoing research is focused towards the synthesis of repair mortars with physico-chemical compatibility to the original ones by using natural raw materials. Methodologically, the first step is the detailed character-

ization of the original mortars, and then, using this information, repair mortars are manufactured. Finally, these repair mortars are characterized in order to assess their suitability for the application.

This study is part of a wider project, which includes the systematic physico-chemical characterization of the historical mortars in Crete, as well as evaluation and assessment of new restoration mortars [2]. Here, the characterization of original mortars from a Venetian Villa in Chania, Crete, and the new synthesized mortars for its restoration are presented as case study. The Venetian Villa at Rodopos is situated in the hinterland of the Chania area and is an important example of the Venetian architecture in rural areas. It was built during the 15th century and the most important interventions were carried out during the 20th century, when the villagers, keeping most of its important elements, transformed the villa into a farmhouse.

The main reasons of deterioration of the construction materials, so far, are salt crystallization, water and salt solutions movement through walls by capillarity and

\* Corresponding author. Tel.: +30 28210 44418; fax: +30 28210 94487.

E-mail addresses: [Noni.Maravelaki@keepka.culture.gr](mailto:Noni.Maravelaki@keepka.culture.gr),  
[nmaravel@electronics.tuc.gr](mailto:nmaravel@electronics.tuc.gr) (P. Maravelaki-Kalaitzaki).

previous transformations which took place during the 20th century. The use of cement mortars in the villa during previous treatments induced severe damage to the adjacent stone blocks. The most common decay patterns are extensive voids and loss of material of the binding mortar. Conservation works require among other actions, repointing of masonry and filling of larger voids. During the year 2000, the 28th Ephorate of Byzantine Antiquities supervised and implemented a funded restoration project of the villa.

Taking into account the basic requirements of a conservation intervention, it was absolutely essential to carry out a thorough and vigorous technical evaluation of the conservation materials [3]. Therefore, in order to design compatible restoration mortars, it was necessary to characterize in detail in mineralogical and chemical terms and to assess the physical and mechanical properties of both the original and repair mortars. Furthermore, an assessment of the performance of the restoration mortars, under real environmental conditions simulated in the laboratory, was required [4].

Besides the physico-chemical compatibility, the proposed repair mortars were manufactured and tested having in mind the following principles: they should not release soluble salts or harmful by-products in the historic masonry, and they should not be stronger than the building stones and excessively stronger than the original mortar.

This study presents the results obtained from (a) the characterization of the original mortars, (b) the design and characterization of repair mortars and (c) the evaluation and monitoring of the proposed repair mortars and plasters used in the restoration of the villa.

## 2. Materials and methods

Fifteen samples of mortars and plasters were selected for this study. Samples were taken from the upper parts of the villa to avoid such phenomena caused by capillary rise. The sampling was carried out by chisel on the external and internal portion of joints including both altered and non-altered material. The analyses were carried out in a significant quantity of samples in order to avoid errors caused by heterogeneity.

It was generally observed that decay patterns encountered in original mortars located in areas previously treated with cement-based mortars. Aiming at detecting the raw materials of the non-altered original mortars, special attention was devoted to sample mortars not having been located in areas adjacent to interventions with cement-based mortars. All the analyses were performed on the internal non-altered portion of joints. Conductivity measurements were carried out in the external portion of mortars (up to 3 cm of depth from the surface) in order to ascertain environmental influences [5].

In order to obtain information about single components and their grain-size distribution, mortar samples were

smoothly separated and sieved through ISO 565 series of sieves. This enables estimation of the proportions of binder/aggregate within the mortar. The most significant fraction of the grain-size distribution, for the aim of this research, is that of  $<63\ \mu\text{m}$  consisting mostly of the binder. Sometimes, however, small quantities of fine aggregate grain inert could be detected in this fraction [2].

Original mortar samples were studied using the following methods and instrumental techniques:

- X-ray diffraction (XRD) analysis of finely pulverized samples was performed with a Siemens D-500 diffractometer working with the Cu K $\alpha$  radiation ( $\lambda=1.5418\ \text{\AA}$ ), and graphite monochromator in the diffracted beam, at 1.5 kW. Spectra were taken from  $4^\circ$  to  $60^\circ\ 2\theta$  at about  $1.8^\circ\ 2\theta/\text{min}$  (step size= $0.03^\circ\ 2\theta$ ; time=1 s).
- Thermal analysis (DSC/TG, Netzsch Sta 1090) was additionally performed to determine the chemical characteristics of the mortars by an appropriate analytical procedure [6]. Samples were heated in static air atmosphere up to a temperature of  $1000^\circ\text{C}$  at a rate of  $10^\circ\text{C}/\text{min}$  to obtain simultaneously the TG and DSC traces.
- Infrared spectroscopy (FTIR, Perkin-Elmer 1000) was used to obtain qualitative information, from a chemical point of view, on some of the characteristic compounds contained in mortar (calcium and magnesium hydroxides and carbonates, gypsum, etc.) and for determining the presence of salts (nitrates, sulfates, oxalates, etc.) as well as organic compounds. The spectra were recorded with a spectral resolution of  $4\ \text{cm}^{-1}$ , and 250 consecutive scans were added and averaged before Fourier transform in order to obtain a good signal-to-noise ratio.
- Calcimetry (Dietrich–Frühling gas volumetric method) was used to determine  $\text{CO}_2$  and to compare it with the results of thermal analysis. The aggregates of the studied mortars were also analyzed using the Dietrich–Frühling gas volumetric method to determine the total  $\text{CO}_2$  content.
- Scanning electron microscopy (SEM) with energy-dispersive X-ray analysis (JEOL 5310) facility provided information on the mineral morphology, crystal size, chemical composition and formed phases.
- Chemical analysis of the principal components was carried out by attack with a sodium carbonate–borax alkaline flux and the subsequent analysis of the elements by traditional chemical methods. The analysis of calcium and magnesium was carried out using a titration with ethylenediaminetetraacetic acid (EDTA), as well as murexide and eriochrome black T (eBT) as indicators. The amounts of  $\text{Fe}_2\text{O}_3$  and  $\text{Al}_2\text{O}_3$  were determined by titration using barium diphenylaminosulphonate and ditizon as indicators. In order to assess the presence of hydraulic compounds, crushed mortar was attacked by HCl (1:5) 2 M at room temperature for 3 h [2]. The amounts of  $\text{SiO}_2$  in the acid-soluble fraction were

determined using atomic emission spectrometry (AES, Perkin-Elmer 3030).

- Conductivity measurements of the water-soluble fraction of mortars and binders estimated the amount of salts present [5].

The performance assessment study of the new restoration mortars included the following:

- Characterization of the mechanical properties of the restoration mortars through determination of the compressive strength ( $f_{mc,k}$ ) and the modulus of elasticity [7]. Compressive strength of cubic specimens ( $5 \times 5 \times 5$  cm) was studied after one month and 1-year setting period. Compression tests were carried out on six samples. Testing was performed with a universal mechanical tester—INSTRON 1026—at a loading rate of  $109 \mu\text{m}/\text{min}$ .
- Water absorption measurements were carried out on three cubic samples of dimension  $5 \times 5 \times 5$  cm each of the restoration mortars. The test was performed according to the methodology described in the Italian protocol Norma UNI 10859 [8]. The capillary water absorption coefficient of a material is interpreted as the angular coefficient of the rectilinear part of the capillary absorption curve. The same measurement was also carried out on specially modulated samples of the original mortar and stone.
- Mercury porosimetry (Carlo Erba 4000) was also employed to obtain the porosity and pore-size distribution of the restoration mortars as well as the original mortar and stone.

### 3. Results and discussion

#### 3.1. Analysis of the original mortars

A macroscopic examination of the sampled material has identified three types of mortars differing in the composition, texture and color and one type of plaster: (a) the first

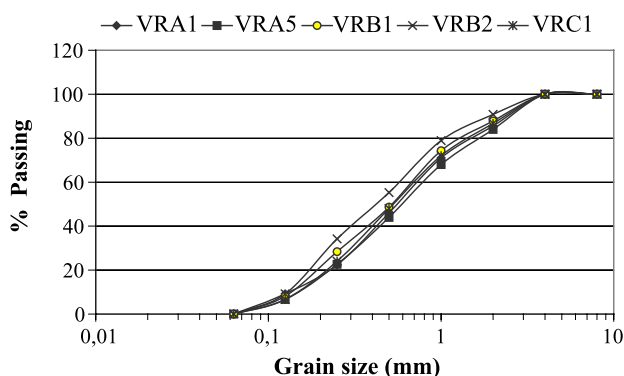


Fig. 1. Grain-size distribution of the aggregates in the original mortars.

Table 1

Mortar description and mineralogical composition

Sample	Description	Composition
VRA1 m	Mortar with beige color consisting of lime, crushed brick and sand	Calcite, Quartz, Magnesite, Dolomite, Halite
VRA1 b	Binder of whitish color	Calcite, Quartz, Magnesite, Halite
VRA2 pl	Plaster with lime, crushed brick and sand	Calcite, Quartz, Magnesite, Halite
VRA3 m	Mortar with brown color consisting of lime, clays and sand	Calcite, Quartz, Illite
VRA4 m	Mortar with beige color consisting of lime, crushed brick and sand	Calcite, Quartz, Magnesite, Dolomite, Halite, Illite
VRA5 m	Mortar with gray color consisting of lime and sand	Calcite, Quartz, Dolomite, Halite
VRA5 b	Binder of whitish color	Calcite, Quartz, Halite
VRB1 m	Mortar with pink-brown color consisting of lime, crushed brick and sand	Calcite, Quartz, Illite, Halite, Dolomite, Magnesite
VRB2 m	Mortar with pink-brown color consisting of lime, crushed brick and sand	Calcite, Dolomite, Halite, Quartz, Illite
VRC1 m	Mortar with brown color consisting of lime and sand	Calcite, Halite, Dolomite, Quartz, Muscovite
VRC2 m	Mortar with brown-red color consisting of lime, clays and sand	Illite, Quartz

m: mortar; b: binder; pl: plaster.

Calcite (5-0586); Quartz (5-0490); Dolomite (36-0426); Muscovite (6-0263); Halite (5-0628); Illite (29-1496, 26-0911); Magnesite (8-0479).

type of mortars contained lime, clays and sand, (b) the second one contained lime, crushed brick and sand and (c) the third one contained lime and sand. The latter, was characterized by high hardness and was hardly detached. All plasters contain lime, as well as sand and crushed brick of fine grain size.

The grain-size distribution of the aggregates of the above classified mortars, after separation and sieving, is shown in Fig. 1. From Fig. 1, it is apparent that: (a) the grain-size distribution of the aggregate in the original mortars ranges between 0.125 and 0.900 mm and (b) about 45% of sand has size smaller than 0.5 mm. The binding material content, conventionally defined as the whole mortar passing—after being suitably prepared—through the 0.125 mm sieve, ranges between 30% and 25%. The binder/aggregate ratio can be obtained by dividing the mass of the mortar sample passing the 0.125 mm sieve by the mass retained by the same sieve. Therefore, the grain-size distribution of the whole mortar enables estimation of the binder/aggregate ratio from 1:2 up to 1:3 per weight of mortars.

According to the results of the gas volumetric  $\text{CO}_2$  determination of the aggregates, a large variety of aggregates were observed, ranging from calcitic and dolomitic to siliceous, differing sometimes not only among the various mortars but even within the same mortar. In general, crushed

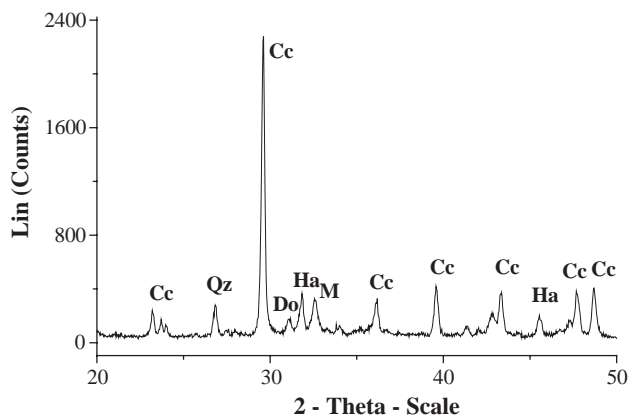


Fig. 2. XRD of an original magnesian mortar. Cc: calcite; Qz: quartz; Do: dolomite; Ha: halite and M: magnesite.

stone of calcitic and dolomitic nature, exhibiting diameters from 1 up to 2 mm and sand of siliceous nature were employed as aggregates.

Mineralogical characterization of the aggregates and binder was obtained by means of XRD and FTIR analyses. The qualitative results of the XRD analysis are presented in Table 1. The dominant phases are calcite ( $\text{CaCO}_3$ ) together with magnesite ( $\text{MgCO}_3$ ), dolomite [ $\text{CaMg}(\text{CO}_3)_2$ ], halite ( $\text{NaCl}$ ) and quartz ( $\text{SiO}_2$ ). A representative XRD spectrum of the mortar is given in Fig. 2 with dominant phases calcite, quartz, dolomite, halite and magnesite.

The FTIR analysis revealed compounds developed in the historical mortars over years during curing and weathering processes. In particular, the second infrared derivative has been taken into consideration, since this allows discrimination of overlapping bands even between minerals with similar absorptions. Fig. 3 illustrates the infrared spectrum (a) and the infrared second derivative (b) of the binder of a mortar with crushed brick. Magnesite (1432, 875 and 746

$\text{cm}^{-1}$ ), nesquehonite ( $\text{MgCO}_3 \cdot 3\text{H}_2\text{O}$ : 1513, 1471, 875 and 746  $\text{cm}^{-1}$ ), potassium nitrate ( $\text{KNO}_3$ : 1384  $\text{cm}^{-1}$ ), quartz (1081 and 792  $\text{cm}^{-1}$ ) and calcite (1432, 875 and 706  $\text{cm}^{-1}$ ) were identified [9].

The infrared spectrum (Fig. 4a) and the second derivative (Fig. 4b) of the binder of a plaster revealed the presence of hydromagnesite [ $4\text{MgCO}_3 \cdot \text{Mg}(\text{OH})_2 \cdot 4\text{H}_2\text{O}$ : 3648, 3516, 3450, 1484, 1425, 1121, 877, 794, 746, 595 and 435  $\text{cm}^{-1}$ ] and calcite as illustrated in Fig. 4. The development of hydromagnesite results from the hydration and carbonation of  $\text{MgO}$  in the lime paste in a moist  $\text{CO}_2$  atmosphere [10].

The infrared analysis also contributed to the aggregate characterization. In Fig. 5, the infrared spectra of a crushed-stone aggregate (a) and aggregates of siliceous sand (b) are reported, where the presence of dolomite (1436, 878 and 726  $\text{cm}^{-1}$ ) and quartz (1167, 1081, 790–778, 691 and 460  $\text{cm}^{-1}$ ) is evident, respectively.

Halite and potassium nitrate identified in the mortars originate from the use of coastal sand and the presence of animals in the villa, respectively.

Table 2 shows the results of the thermal analysis carried out on a temperature range of 30–1000  $^{\circ}\text{C}$ . The weight loss at temperature  $<120$   $^{\circ}\text{C}$  is due to the release of hygroscopic water. The weight loss in the range of 120–400  $^{\circ}\text{C}$  is associated with the water bound to magnesium carbonate compounds and clay minerals. The weight loss in the range of 400–550  $^{\circ}\text{C}$  is due to the decarbonation of magnesium carbonates, while the weight loss in the range of  $>600$  is associated with the decarbonation of calcium carbonate.

Table 3 shows the results of the complete chemical attack in mortars, binders and plasters, as well as the determination of total  $\text{CO}_2$ , total and acid-soluble  $\text{SiO}_2$  and conductivity. The results of the chemical analysis revealed a significant amount of  $\text{MgO}$  due to the presence of some dolomitic aggregates and magnesian lime. A  $\text{CaO/MgO}$  ratio of 1.9

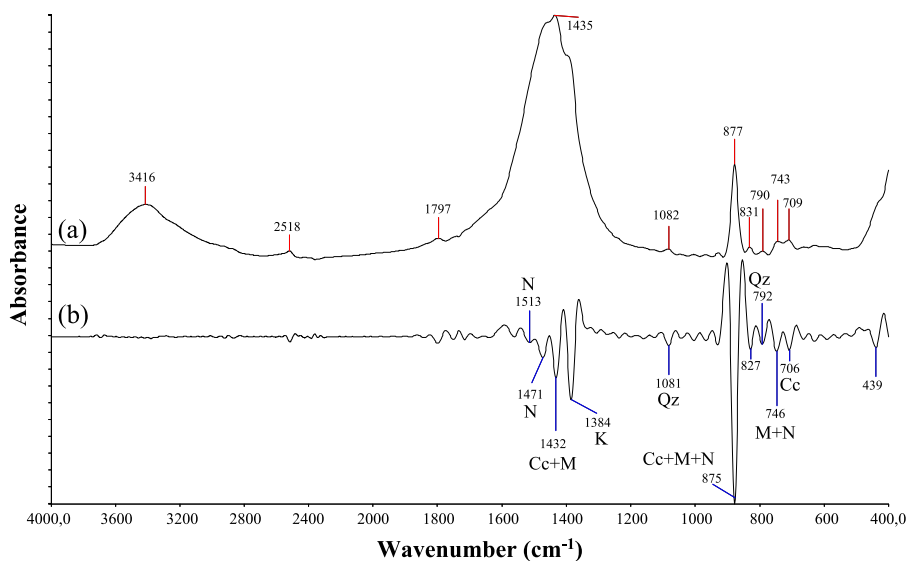


Fig. 3. Infrared spectrum (a) and infrared second derivative (b) of the binder of a mortar with crushed brick. Cc: calcite; Qz: quartz; M: magnesite; N: nesquehonite and K: potassium nitrate.

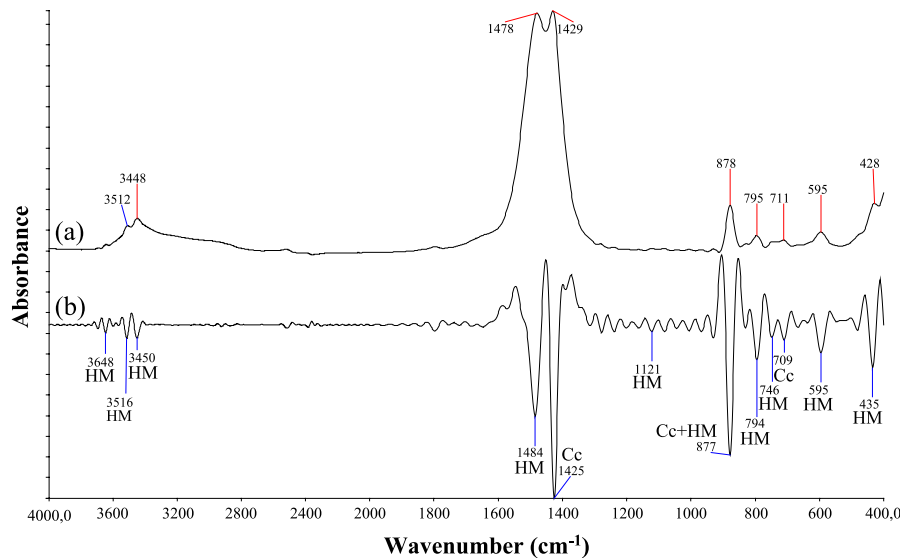


Fig. 4. Infrared spectrum (a) and infrared second derivative (b) of the binder of a plaster. HM: hydromagnesite and Cc: calcite.

was calculated in the mortars, while in the binders this ratio varies from 1.7 up to 2.5. The studied mortars differ from previously analyzed mortars in Crete as far as MgO content is concerned. The ancient crushed brick-lime mortars in Crete, regardless of the historic period, showed an average of 1.5 wt.% MgO, while the magnesian mortars of this study show a quantity of ~13 wt.% MgO [2].

The quantity of the detected SiO<sub>2</sub> is related to the presence of siliceous sand and/or the ceramics used in the mortar matrix (see Table 3). In general, mortars with clay minerals show large amounts of total SiO<sub>2</sub>, while the low amount of soluble SiO<sub>2</sub> indicates that they exhibit a low degree of hydraulicity. Noticeable amount of SiO<sub>2</sub> was also detected in the binders of the studied mortars (VRA1 and VRA5) because of the inevitable presence of clays, fine crushed brick and siliceous sand in the fraction of less

than 0.063  $\mu\text{m}$ , where the major part of the binder is included.

The results of the determination of total conductivity showed that mortars and plasters were extensively affected by salt contamination (see Table 3). This finding further supports that strength and weathering resistance are decreased in the original mortars. Therefore, the replacement of part of the original mortars was essential.

The SEM analysis on fractured surfaces of mortars reveals the microstructure of different phases. In Fig. 6a, the SEM photomicrograph of a binder conglomerate is reported showing a very good compactness and low amount of micropores. The SEM-EDS microanalysis performed in the same area has mainly identified Ca and Mg (Fig. 6b). This analysis gives an elemental proportion of Ca/Mg equal to 2.1, which in turn corresponds to the proportion of CaO/

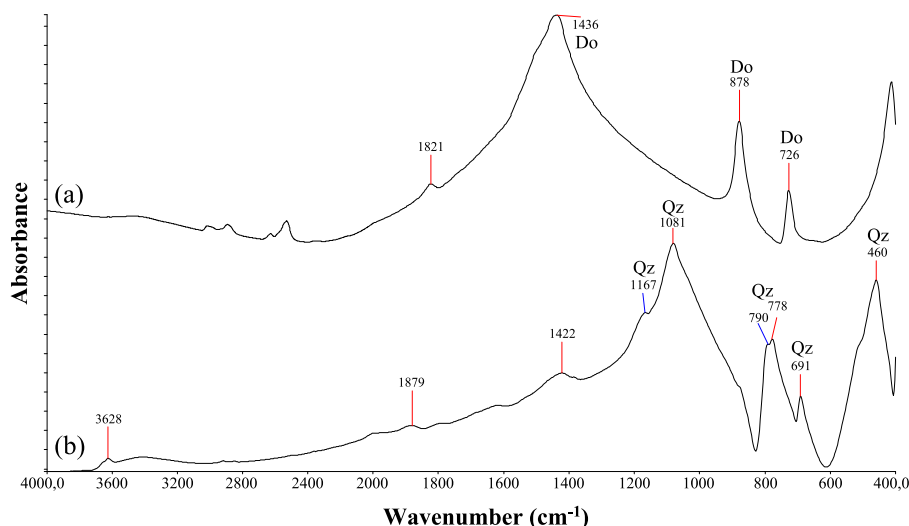


Fig. 5. Infrared spectra of a crushed-stone aggregate (a) with dolomite (Do) and siliceous sand aggregates (b) with quartz (Qz).



Table 2  
Results of thermal analysis

Sample	Weight loss per temperature range (%)			
	<120 °C	120–400 °C	400–550 °C	>600 °C
VRA1 b	2.44	6.32	14.43	18.03
VRA2 pl	2.38	6.14	19.76	20.79
VRA3 m	1.42	3.19		20.88
VRA5 m	1.75	4.33	10.43	15.44
VRA5 b	1.77	5.58	12.07	21.20

m: mortar; b: binder, pl: plaster.

MgO calculated from the results of chemical and thermal analyses.

The analysis of the studied samples pointed out that magnesian lime mortars were employed in the construction of villa. This is the first case that magnesian mortars were detected as construction materials throughout the centuries in Greece. Since dolomitic stones have been located in the local area of the villa, it seems reasonable that dolomites have been included as prime materials for the production of lime.

### 3.2. Design of restoration mortar and experimental procedure

Aiming to the design of new restoration mortars, compatibility involves aspects, such as philosophical and ethical issues, physico-chemical and mechanical properties, interaction of mortars with masonry, protection of original materials and prevention of deterioration mechanisms. In every case, the final product must be durable and easy in application. The main directives for the design of repair mortars suggest that there is a need for strengthened mortars for the replacement of both deteriorated joint mortars and cement mortars previously used and the use of raw materials of similar chemical composition [3].

Considering that magnesian lime is not produced in Greece and the requirements for improved strength, the binding material of mixtures should be either hydraulic lime or lime mixed with some pozzolan. The latter option was rejected as their performance and mechanical properties are for a long time strongly depended on the setting conditions (temperature and relative humidity), the quality of pozzolan and the environmental fluctuations [11]. Furthermore, bibliographic search indicated that there is a lack of studies on the performance of mortars made of magnesian lime.

On the other hand, a variety of studies are dedicated to the assessment and evaluation of mortars containing hydraulic lime. Nowadays, hydraulic lime-based mortars are being assessed in laboratory experiments and are also employed as repair mortars in historic masonry [12–15]. This ongoing research both in laboratory and on site provided encouraging results and recommended the use of natural hydraulic lime in restoration projects. Hydraulic lime as binding material also behaved satisfactorily in several conservation applications conducted in the framework of the restoration procedures of our Ephorate. Therefore, laboratory and on-site applications suggested the use of hydraulic lime for the design of the repair mortar.

The raw materials finally selected for the design of the repair mortars and plasters consist of natural hydraulic lime with pozzolanic additions (NHL-Z 3.5) as binding material and aggregates of siliceous sand and crushed brick. The aggregates were selected in view of both emulation of nature of the examined aggregates and avoidance of chemical interaction between aggregates and binder. In particular, dolomitic aggregates were avoided due to expansion and crack observed in concrete made of high-alkali Portland cement and dolomitic limestone aggregate, according to the dedolomitization reaction [16]. The characteristics of the raw materials employed in the mortar synthesis are reported in Table 4. The aggregates exhibit

Table 3  
Results of the complete chemical analysis

	%CaO <sup>a</sup>	%MgO <sup>a</sup>	%Al <sub>2</sub> O <sub>3</sub> <sup>a</sup>	%Fe <sub>2</sub> O <sub>3</sub> <sup>a</sup>	Percent total SiO <sub>2</sub> <sup>a</sup>	Percent sol. SiO <sub>2</sub> <sup>b</sup>	%CO <sub>2</sub> (DF) <sup>c</sup>	Con (μS/cm)
VRA1 m	20.98	11.05	1.12	0.22	12.14	0.42	29.66	251.70
VRA1 b	21.14	12.54	1.23	0.21	8.12	0.32	30.43	265.15
VRA2 pl	27.98	13.98	0.42	0.18	5.62	nd	38.33	102.46
VRA3 m	26.57	nd	6.12	1.23	30.58	nd	19.61	112.69
VRA4 m	21.56	11.35	2.86	0.53	16.23	0.21	28.30	160.23
VRA5 m	19.14	10.12	3.14	0.38	25.14	0.26	25.13	81.25
VRA5 b	25.31	10.14	0.98	0.89	14.05	0.14	31.45	94.70
VRB1 m	21.27	12.14	1.52	0.57	15.21	0.21	29.02	220.83
VRB2 m	22.80	11.84	1.47	0.22	15.36	nd	32.48	154.92
VRC1 m	21.38	11.25	2.13	0.41	20.13	0.19	29.18	108.90
VRC2 m	1.11	nd	12.45	1.43	62.47	nd	0.87	61.93

Percentages related to original dry mortar.

m: mortar; b: binder; pl: plaster.

nd: non-detectable.

<sup>a</sup> Sodium carbonate–borax alkaline flux.

<sup>b</sup> Attack by HCl (1:5) 2 M at room temperature for 3 h.

<sup>c</sup> Dietrich–Frühling gas volumetric method.

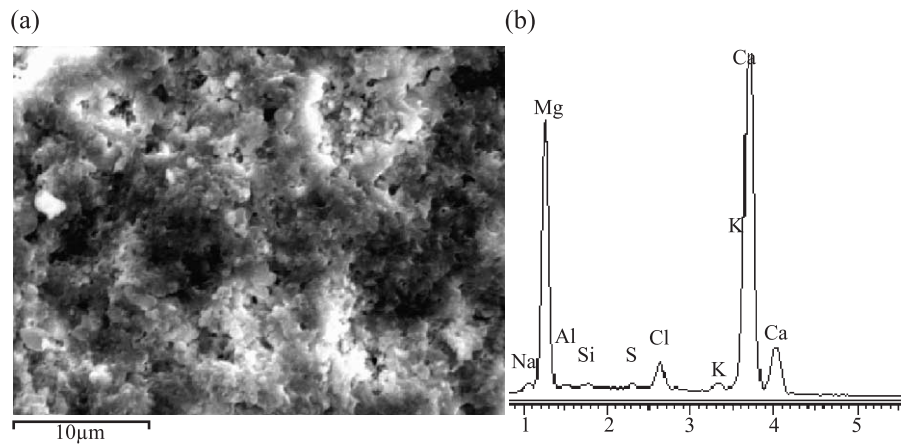


Fig. 6. SEM photomicrograph of a binder conglomerate (a) at high magnification (scale=10  $\mu\text{m}$ ) and corresponding SEM-EDS spectrum (b) (full scale=14,880 counts).

similar particle-size distribution to that detected in the original mortars.

Different mixtures of mortars were prepared and tested both in laboratory and on site, aiming to the assessment of optimum workability. Good workability was achieved by mixing hydraulic lime and siliceous sand in a ratio of 6:14 by weight, as well as hydraulic lime, siliceous sand and crushed brick in a ratio of 6:14:1 by weight, for joint and plaster mortars, respectively (see Table 4). The water/binder ratio for mortars and plasters was 0.54 and 0.66, respectively. According to the experiments, this amount of water was necessary in order to achieve normal consistency and a good workability (measured by the flow table test [17]).

Physical and mechanical properties of joint mortars were studied in laboratory, while the performance of plasters was estimated on site, at selected areas of the building. The test specimens were placed in controlled chamber of  $95 \pm 1\%$  relative humidity and  $20 \pm 1^\circ\text{C}$  for 3 days and then stored in air-conditioned room at  $20 \pm 1^\circ\text{C}$  and  $60 \pm 1\%$  relative humidity until their evaluation [18].

Table 4  
Characteristics of the raw materials

Raw materials, mortar and plaster	Characteristics
Natural hydraulic lime (NHL)	65% CaO, 11% SiO <sub>2</sub> , 12% CO <sub>2</sub> , 9% H <sub>2</sub> O, 0.8% Al <sub>2</sub> O <sub>3</sub> +Fe <sub>2</sub> O <sub>3</sub> , 0.5% MgO, 0.2% K <sub>2</sub> O+Na <sub>2</sub> O
Sand	NHL-Z 3.5 according to CEN prEN 459-1 Siliceous sand 8.4% CaO, 75.3% SiO <sub>2</sub> , 4.9% Al <sub>2</sub> O <sub>3</sub> , 0.5% Fe <sub>2</sub> O <sub>3</sub> , 1.5% MgO, 0.7% K <sub>2</sub> O, 0.9% Na <sub>2</sub> O, 4.2% CO <sub>2</sub>
Crushed brick	Ceramic aggregates 3.1% CaO, 59% SiO <sub>2</sub> , 17.4% Al <sub>2</sub> O <sub>3</sub> , 9.1% Fe <sub>2</sub> O <sub>3</sub> , 2.5% MgO, 2.2% K <sub>2</sub> O, 1.1% Na <sub>2</sub> O, 2.9% CO <sub>2</sub>
Mortar	NHL:Sand=6:14, Water/Binder=0.54, Flow test=155 mm
Plaster	NHL:Sand:Crushed brick=6:14:1, Water/Binder=0.66, Flow test=155 mm

### 3.3. Evaluation of the characteristics of the proposed repair mortars

Table 5 reports the water absorption coefficients (CA) determined by the capillary water absorption action for the repair mortar, an original magnesian mortar and an original stone of the villa (a bioclastic limestone). The repair mortar shows almost similar ability to absorb water by capillary action to the stone and to the original magnesian mortar. Building materials with similar capillary absorption coefficients, as in our case, behave accordingly, as far as moisture movement and evaporation are concerned.

The porosity and pore-size distribution are important factors to consider when studying the compatibility between ancient and restored structures. A total porosity of 26.2% is calculated for the repair mortar, while this value ranges from 24% up to 30% for the stone and from 30% up to 40% for the original mortar. Fig. 7 depicts the total porosity (cumulative volume) as a function of the pore-size distribution for the stone (a), original (b) and repair mortar

Table 5  
Mechanical and physical properties of the proposed repair mortars calculated after curing of 1 and 12 months

	Compressive strength (N/mm <sup>2</sup> )	Modulus of elasticity (N/mm <sup>2</sup> )	Capillary water absorption coefficient (CA) (mg/cm <sup>2</sup> s <sup>1/2</sup> )	Porosity (%)
Repair mortar (1 month)	3.48 ( $\pm 0.07$ )	$7.12 \times 10^3$ ( $\pm 0.10$ )	24.16 ( $\pm 0.12$ )	nd
Repair mortar (12 months)	5.67 ( $\pm 0.03$ )	$8.94 \times 10^3$ ( $\pm 0.19$ )	nd	26.23 ( $\pm 0.14$ )
Original mortar	nd	nd	28.51 ( $\pm 0.42$ )	30–40
Stone	10.09 ( $\pm 0.25$ )	$9.30 \times 10^3$ ( $\pm 0.21$ )	31.32 ( $\pm 0.17$ )	24–30

nd: not determined.

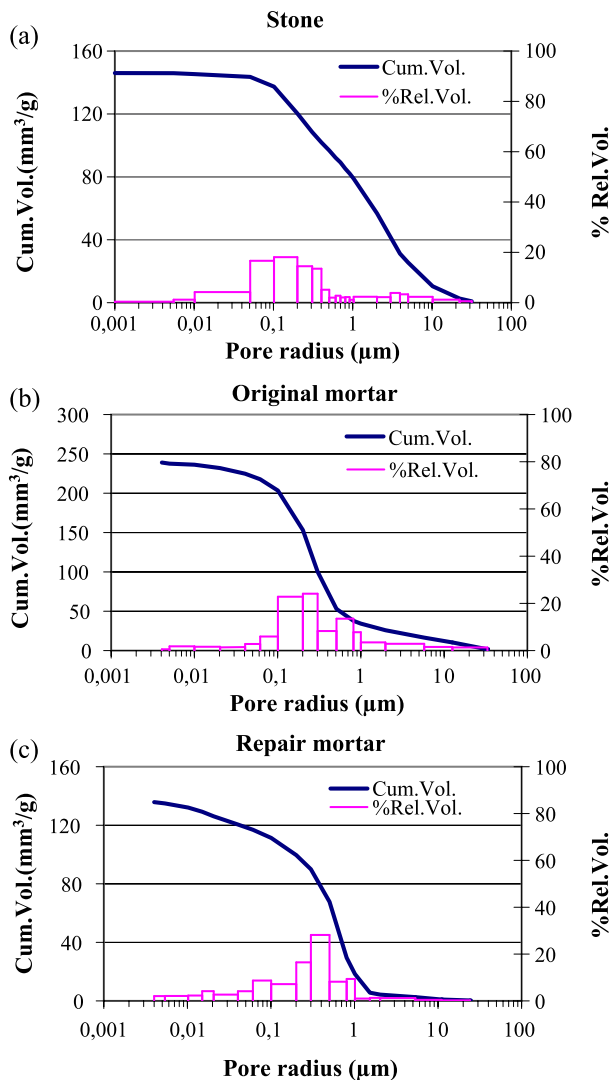


Fig. 7. Total porosity (cumulative volume) as a function of pore radius distribution for the stone (a), original (b) and repair mortar (c).

(c). The original and repair mortar, as well as the stone, exhibit similar pore radius distribution with radius size between 0.1 and 1 μm.

The microstructure strongly influences the water movement and evaporation, as well as the salt crystallization. The failure of the cement-based mortars is mainly due to their totally different pore-size distributions from the stone and original mortars. The cement-based mortars are characterized by pores with radius <0.01 μm, and therefore these small pores direct saline solutions towards the stone. Furthermore, in cement mortars, cracks were observed due to high crystallization pressures of salts [19]. The similar pore-size distribution between stone, original and repair mortar indicates that compatibility exists and proves the suitability of the mortar for such an application.

Compressive strength and the evaluation of modulus of elasticity values are also presented in Table 5. The compressive strength is doubled after 12 months of curing. In this period, the mortars lose the water excess. The

increase in strength is also due to the hydration of several hydraulic compounds which form hydrated calcium silicates and aluminates. Furthermore, the elimination or reduction of  $\text{Ca(OH)}_2$  by reaction with pozzolan and/or carbonation can result in greatly enhanced durability and strength. The repair mortar exhibits lower compressive strength than the stone and similar modulus of elasticity to the stone. This property is suitable for the intended use of the repair mortar to join the original mortars and the stone blocks.

### 3.4. Application of the proposed hydraulic mortars in the villa

Laboratory and on-site experiments demonstrated that the proposed repair mortar based on hydraulic lime could effectively be employed for the restoration of the villa. In 2001, after preliminary removal of deteriorated original mortars as well as cement-based mortars and plasters, it was decided to proceed to the intervention by employing the proposed hydraulic lime mortars. After 3 years of application, no decay patterns are observed and the applied mortar seems to suit well to the original structure. It is important to emphasize that although the roof has not been repaired yet and therefore the shell of the villa has been subjected to the rain action, no decay patterns are observed. The repair mortar is characterized by consistency and fits well to the structure, while no cracks or efflorescence has been observed.

In order to assess the neo-formed compounds of the applied mortars and especially the presence of soluble salts, FTIR and XRD analyses were carried out in a repair mortar sampled from the villa. The results reveal the absence of soluble salts, such as halite and potassium nitrate, and the presence of hydraulic compounds after the hydration of calcium silicates. Fig. 8 illustrates the infrared spectrum of the repair mortar after a 3-year application, where absorptions attributed to hydraulic compounds are evident. In particular, the broad band at  $1000\text{--}970\text{ cm}^{-1}$  arises from C–S–H vibrations [20,21]; additionally, the

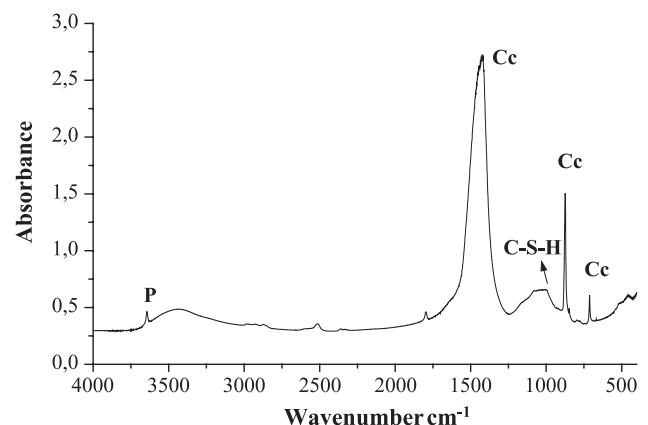


Fig. 8. Infrared spectrum of the repair mortar after a 3-year application with calcite (Cc), portlandite (P) and adsorptions attributed to hydration of hydraulic compounds (C–S–H vibrations: broad band at  $1000\text{--}970\text{ cm}^{-1}$ ).



band at  $3644\text{ cm}^{-1}$  is attributed to the OH of portlandite, indicating that a complete carbonation has not been achieved yet. The hydraulic compounds together with the lack of soluble salts improved the mortar performance. It can be stated that chemical, physical and structural compatibility between original structure and repair mortar was achieved. Therefore, the conservation intervention with the employment of the proposed hydraulic lime mortars can be considered effective.

#### 4. Conclusions

This study reports the first case of detection of magnesian lime mortars in the historic masonry of Greece. Magnesian lime mortars were detected in a Venetian Villa at Rodopos, Chania, Crete, Greece, in an area where dolomitic stones exist. The main reasons of the original mortar replacement were its natural decay and the previous interventions with cement-based materials, which resulted in advancing the state of decay of the whole structure. In the present conservation application, the main focus was to achieve compatibility between old and restoration materials by using raw materials, similar to the old ones. However, the lack of laboratory and on-site issues on the performance of magnesian lime mortars suggested the use of the well-established natural hydraulic lime.

The proposed repair mortar and plaster consist of natural hydraulic lime as binding material, while aggregates of siliceous sand and crushed brick are used. The repair mortar shows similar pore-size distribution and capillary absorption coefficient with both the original mortar and stone. The repair mortar exhibits lower compressive strength than the stone, but this value lies in acceptable ranges for such an application, since the repair mortars exhibit similar modulus of elasticity to the stone. The absence of soluble salts in the repair mortar after a 3-year application period, together with the development of hydraulic phases like calcium silicate hydrates, and the observed consistency between old and repaired structure further encourage the employment of hydraulic lime mortars.

#### Acknowledgements

The authors would like to thank the Mayor of Kolymbari P. Polychronidis, the Consultant of the Association for the Restoration of Kolymbari Monuments C. Protopapadakis and the Director of the 28th Ephorate of Byzantine and Post-Byzantine Antiquities M. Andrianakis for supporting this study. A special acknowledgement is devoted to the TITAN Cement Industry for providing the DSC/TG facility, the Department of Conservation of Antiquities and Works of Art of TEI Athens for providing the SEM facility, as well as to Prof. G. Biscontin of the Venice University for the invaluable information provided during this study.

#### References

- [1] A. Moropoulou, P. Maravelaki-Kalaitzaki, M. Borboudakis, A. Bakolas, P. Michailidis, M. Chronopoulos, Historic mortars technologies in Crete and guidelines for compatible restoration mortars, in: G. Biscontin, A. Moropoulou, M. Erdik, J.D. Rodrigues (Eds.), PACT, Revue du groupe europeen d'etudes pour les techniques physiques, chimiques, biologiques et mathematiques appliques a l'archeologie, Compatible Materials for the Protection of European Cultural Heritage, Technical Chamber of Greece, Athens, vol. 55, 1998, pp. 55–72.
- [2] P. Maravelaki-Kalaitzaki, A. Bakolas, A. Moropoulou, Physico-chemical study of Cretan ancient mortars, *Cem. Concr. Res.* 33 (2003) 651–661.
- [3] A. Moropoulou, Reverse engineering to discover traditional technologies: a proper approach for compatible engineering mortars, in: G. Biscontin, A. Moropoulou, M. Erdik, J.D. Rodrigues (Eds.), PACT, Revue du groupe europeen d'etudes pour les techniques physiques, chimiques, biologiques et mathematiques appliques a l'archeologie, Compatible Materials for the Protection of European Cultural Heritage, Technical Chamber of Greece, Athens, vol. 58, 2000, pp. 81–107.
- [4] L. Binda, G. Baronio, C. Tedeschi, Experimental study on the mechanical role of thick mortar joints in reproduced Byzantine masonry, in: P. Bartos, C. Groot, J.J. Hughes (Eds.), International RILEM Workshop on Historic Mortars: Characteristics and Tests, RILEM Publications, Cachan Cedex, France, 2000, pp. 227–247.
- [5] UNI 11087 Protocol, Cultural heritage—natural and artificial stones—determination of soluble salts content, 2003.
- [6] A. Bakolas, G. Biscontin, A. Moropoulou, E. Zendri, Characterization of structural Byzantine mortars by thermogravimetric analysis, *Thermochim. Acta* 321 (1998) 151–160.
- [7] G.E. Brown, Testing of concretes, mortars, plasters and stuccos, *Archaeomaterials* 4 (1990) 185–191.
- [8] UNI 10859 Protocol, Cultural heritage—natural and artificial stones—determination of water absorption by capillarity, 2000.
- [9] V.C. Farmer, *Infrared Spectra of Minerals*, Mineralogical Society, London, 1974.
- [10] R.M. Dheilly, A. Bouguerra, B. Beaudoin, J. Tuto, M. Queneudec, Hydromagnesite development in magnesian lime mortars, *Mater. Sci. Eng., A* 268 (1999) 127–131.
- [11] A.E. Charola, F.M.A. Henriques, Hydraulicity in lime mortars revisited, in: P. Bartos, C. Groot, J.J. Hughes (Eds.), International RILEM Workshop on Historic Mortars: Characteristics and Tests, RILEM Publications, Cachan Cedex, France, 2000, pp. 95–104.
- [12] J.M. Teutonico, G. Ashall, E. Garrod, Y. Bates, A comparative study of hydraulic lime-based mortars, in: P. Bartos, C. Groot, J.J. Hughes (Eds.), International RILEM Workshop on Historic Mortars: Characteristics and Tests, RILEM Publications, Cachan Cedex, France, 2000, pp. 339–349.
- [13] V. Fassina, M. Favaro, A. Naccari, M. Rigo, Evaluation of compatibility and durability of a hydraulic lime-based plasters applied on brick wall masonry of historical buildings affected by rising damp phenomena, *J. Cult. Herit.* 3 (2002) 45–51.
- [14] A. Moropoulou, A. Bakolas, S. Anagnostopoulou, Composite materials in ancient structures, *Cem. Concr. Compos.* (2004) 295–300.
- [15] A. Moropoulou, A. Bakolas, P. Moundoulas, E. Aggelakopoulou, S. Anagnostopoulou, Strength development and lime reaction in mortars for repairing historic masonry, *Cem. Concr. Compos.* (2004) 2191–2201.
- [16] L. Tong, M. Tang, Expandability of solid-volume-reducing reactions of alkali-magnesite and alkali-dolomite, *Cem., Concr. Aggreg., CCAGDP* 19 (1) (1997) 31–37.
- [17] EN 1015-3, Methods of test of mortar for masonry: Part 3. Determination of consistence of fresh mortar (by flow table), 1999.

- [18] EN 196-1, Methods of testing cement: Part 1. Determination of strength, 1995.
- [19] C. Sabbioni, G. Zappia, C. Riontino, M.T. Blanco-Varela, J. Aguilera, F. Puertas, K. Van Balen, E.E. Toumbakari, Atmospheric deterioration of ancient and modern hydraulic mortars, *Atmos. Environ.* 35 (2001) 539–548.
- [20] S. Martinez-Ramirez, Influence of SO<sub>2</sub> deposition on cement mortar hydration, *Cem. Concr. Res.* 29 (1999) 107–111.
- [21] J. Bensted, S. Prakash Varma, Some applications of the infrared and Raman spectroscopy in cement chemistry, Part 3, *Cem. Technol.* 5 (5) (1974) 378–382.